Vladimir V. Eliseev · Tatiana V. Zinovieva

Nonlinear-elastic strain of underwater pipeline in laying process

Received: 27.06.2011 / Accepted: 11.04.2012

Abstract The contact problem of laying of an underwater pipeline as a nonlinear-elastic rod is formulated and numerically solved. Influence of various factors, i.e., tension, shear, physical nonlinearity of the material, initial angle and depth, is considered. A new formula for hydrostatic loading is derived and used in calculations. Stresses in the pipe, loading on a vessel, form of the sagging part, and contact pressure are determined.

Keywords Nonlinear-elastic rod · Contact problem · Hydrostatic load · Numerical modeling · Finite difference method

1 Introduction

High safety standards of underwater pipelines cause the relevance of mathematical modeling of their stress-strain state [11,12,14,16,17,19,22]. The damage of the pipeline can occur already at the process of its laying from the vessel to the sea bottom. The calculation of arising stress-strain state with account for various factors and nonlinearities is the goal of this study. Linearized problem is formulated and solved in [22].

In the consequence of smallness of relative thickness of the considered pipeline segment (about 10^{-3}), we can use the one-dimensional models of rods as material lines of Euler–Kirchhoff–Cosserat [2,4–6,15, 21]. The calculations show that on the free segment we can restrict ourselves by using the classical nonlinear model without tension and shear. However, to define the contact pressure on the bottom we need to take into account transverse shear [13]. The bottom as a foundation is considered a horizontal plane, rigid and smooth (frictionless). The contact segment boundary is determined from the corresponding matching conditions. For the large depths we must take into account not only geometric nonlinearity, but also physical nonlinearity, because the concrete of the outer layer is not subjected to Hookes law. The computation of hydrostatic load on the pipe calls for special attention. The simplified ideas found in literature [12,16,17,20] can change the solution quantitatively and qualitatively.

The theory and technique of calculation proposed in this work let us optimize the laying process of underwater pipelines without overstress of them at the first stage.

2 Problem formulation and system of equations

The pipeline which is the two-layered curved tube from steel and concrete is modeled as a half-infinite rod. This rod is rigidly fixed at the left end (Fig. 1). The rod having the compliance of bending, tension and shear

Translated from: V.V. Yeliseyev, T.V. Zinovieva. Nonlinear-elastic strain of underwater pipeline in laying process. Computational Continuum Mechanics **5**(1) 70–78 DOI 10.7242/1999-6691/2012.5.1.9

Vladimir V. Eliseev · Tatiana V. Zinovieva
Department of Computer Technology in Mechanical Engineering, Saint-Petersburg State Polytechnic University, Saint-Petersburg, Russia, E-mail: yeliseyev@inbox.ru, tatiana.zinovieva@gmail.ru

is loaded by its own weight and by the external pressure of liquid. The distance between the fixation and the bottom is prescribed, and the length of freely sagging segment is unknown and must be found. We take the straight form of rod in the stress-free state as the pipeline reference configuration.

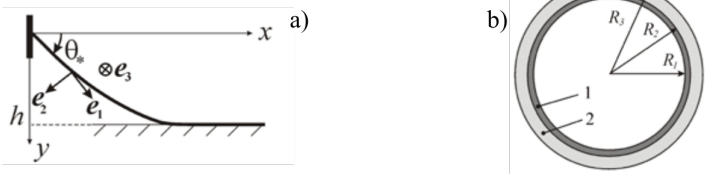

Fig. 1 Scheme of pipeline (a) and its section (b). 1 is steel, 2 is concrete

The geometric form of rod as a material line is determined by the dependence of position vector $\mathbf{r}(s)$ of the points forming this line on the Lagrangian coordinate s. In the initial state it is $\mathbf{r}_0(s)$. Since s is the arc coordinate, the derivative $\mathbf{r}'(s)$ is equal to the tangent unit vector $\mathbf{t}_0$. At the same time we relate the triple of orthogonal unit vectors $\mathbf{e}_i(s)$ with every particle of the rod as the Cosserat line; in the initial state they are usually $\mathbf{e}_{i0} = \mathbf{t}_0(s)$. The vector of curvature and twisting $\boldsymbol{\Omega}(s)$ is determined by the equations $\mathbf{e}_i{}' = \boldsymbol{\Omega} \times \mathbf{e}_i$. The rotation tensor $\hat{\mathbf{P}} \equiv \mathbf{e}_i \mathbf{e}_{i0}$ (we sum up by repeated indices) relates the directing unit vectors before and after the deformation: $\mathbf{e}_i = \hat{\mathbf{P}} \cdot \mathbf{e}_{i0}$.

The system of equations of nonlinear statics of elastic rods has the form [4,6]:

$$\begin{aligned} &\mathbf{Q}' + \mathbf{q} = 0,\ \mathbf{M}' + \mathbf{r}' \times \mathbf{Q} + \mathbf{m} = 0, \\ &\boldsymbol{\kappa} \equiv \boldsymbol{\Omega} - \hat{\mathbf{P}} = \hat{\mathbf{A}} \cdot \mathbf{M} + \hat{\mathbf{C}} \cdot \mathbf{Q},\ \boldsymbol{\Gamma} \equiv \mathbf{r}' - \hat{\mathbf{P}} \cdot \mathbf{r}_0{}' = \hat{\mathbf{B}} \cdot \mathbf{Q} + \mathbf{M} \cdot \hat{\mathbf{C}}. \end{aligned} \tag{1}$$

Here $\mathbf{Q}$, $\mathbf{M}$ are the force and moment vectors in the section with the coordinate s. The first two equations describe the balance of forces and moments with the distributed loads $\mathbf{q}$, $\mathbf{m}$ (force and moment correspondingly), other relations involve the strain vectors $\boldsymbol{\kappa}$, $\boldsymbol{\Gamma}$ and relate them to the force factors using the compliance tensors $\hat{\mathbf{A}}$, $\hat{\mathbf{B}}$, $\hat{\mathbf{C}}$. The whole system of equations (1) can be derived from the principle of virtual work [4–6,21]. The relations of elasticity in the system (1) correspond the physically linear model with quadratic dependence of strain energy $\Pi(\kappa_i, \Gamma_i)$ on its arguments. In the case of physical nonlinearity we have $\mathbf{M} = \mathbf{e}_i\, \partial\Pi/\partial\kappa_i$, $\mathbf{Q} = \mathbf{e}_i\, \partial\Pi/\partial\Gamma_i$ where $\kappa_i \equiv \boldsymbol{\kappa} \cdot \mathbf{e}_i$, $\Gamma_i \equiv \boldsymbol{\Gamma} \cdot \mathbf{e}_i$. The last follows also from the principle of virtual work.

The tensor $\hat{\mathbf{A}}$ characterizes the bending and twisting compliance, the tensor $\hat{\mathbf{B}}$ is the tension and shear compliance, the tensor $\hat{\mathbf{C}}$ describes the cross links. The computation of compliance tensors requires the consideration of the three-dimensional rod model. Herewith solutions of the Saint-Venant problem, the asymptotic method, and the variational approach with approximations in the cross-section are used [4–6,21]. The simplest version of writing the tensors is the following: $\hat{\mathbf{A}} = \sum A_i \mathbf{e}_i \mathbf{e}_i$, $\hat{\mathbf{B}} = \sum B_i \mathbf{e}_i \mathbf{e}_i$, $\hat{\mathbf{C}} = 0$. Here six compliances differ from zero: the twisting compliance A_1, the bending ones A_2, A_3, the tension compliance B_1 and shear ones B_2, B_3.

Then we consider the deformation of the pipeline in the vertical plane xy with $\mathbf{m} = 0$ and with the simplest version of compliance tensors. In the plane xy (see Fig. 1, a) the vectors $\mathbf{Q}$, $\mathbf{q}$, $\mathbf{r}$, $\boldsymbol{\Gamma}$, $\mathbf{e}_1$, $\mathbf{e}_2$ lie. Vectors $\mathbf{M}$, $\boldsymbol{\kappa}$ are perpendicular to the plane (i.e. parallel to the Cartesian axis z with the unit vector $\mathbf{k} = \mathbf{e}_3$). Instead of the rotation tensor it is sufficient to take the angle $\theta(s)$ between the axis x and the unit vector $\mathbf{e}_1$. With this assumptions the equations (1) are simplified:

$$\begin{aligned} &\mathbf{Q}' + \mathbf{q} = 0,\ \mathbf{M}' + \mathbf{k} \cdot \mathbf{r}' \times \mathbf{Q} = 0,\ \theta' = AM,\ \left(A \equiv A_3,\ M = A^{-1}\theta' \equiv A^{-1}\kappa\right), \\ &\mathbf{r}' = \mathbf{e}_1 + \hat{\mathbf{B}} \cdot \mathbf{Q},\ \mathbf{e}_1 = \mathbf{i}\cos\theta + \mathbf{j}\sin\theta,\ \hat{\mathbf{B}} = B_1 \mathbf{e}_1 \mathbf{e}_1 + B_2 \mathbf{e}_2 \mathbf{e}_2,\ \mathbf{e}_2 = -\mathbf{i}\sin\theta + \mathbf{j}\cos\theta. \end{aligned} \tag{2}$$

In the projections on the Cartesian axes x, y, we have the system

$$\begin{aligned} &Q_x{}' + q_x = 0,\ Q_y{}' + q_y = 0,\ M' + x' Q_y - y' Q_x = 0,\ \theta' = AM, \\ &x' = \cos\theta + B_{xx} Q_x + B_{xy} Q_y,\ y' = \sin\theta + B_{yx} Q_x + B_{yy} Q_y, \\ &B_{xx} = B_1 \cos^2\theta + B_2 \sin^2\theta,\ B_{yy} = B_1 \sin^2\theta + B_2 \cos^2\theta, \\ &B_{xy} = (B_1 - B_2)\sin\theta\cos\theta. \end{aligned} \tag{3}$$

3 Contact problem with simplified load

At first we assume, that hydrostatic load is constant. Then

$$q_x = 0,\ q_y = \tilde{w} + \begin{cases} 0, & s < l, \\ -p(s) & s > l \end{cases} \tag{4}$$

where $\tilde{w} = \text{const}$ is the distributed per unit length weight of the pipeline in water [20]. The contact load $p(s)$ and the coordinate $s = l$ of the free (sagging) segment tip are unknown. It is obvious that in the system of equation (2) $Q_x = 0$.

On the contact segment we have:

$$\begin{aligned} &y = h \Rightarrow \sin\theta + B_{yy} Q_y = 0 \Rightarrow Q_y = -\sin\theta / B_{yy}; \\ &p = \tilde{w} + Q_y{}';\ M' + x' Q_y = 0 \Rightarrow \theta'' + A(\cos\theta + B_{xy} Q_y) Q_y = 0 \Rightarrow \theta'' = \left(AB_2 / B_{yy}^2\right) \sin\theta \cos\theta. \end{aligned} \tag{5}$$

Here the equation for $\theta(s)$ permits reduction of order:

$$\theta'^2 + AB_2 / \left[(B_1 - B_2) B_{yy}\right] = \text{const} = A / (B_1 - B_2) \Rightarrow \theta' = -\sqrt{A / B_{yy}} \sin\theta; \tag{6}$$

Herewith we use the condition $\theta(\infty) = 0$.

The equation (6) can be integrated in quadratures, however the simpler way is to integrate it numerically. At the start of the contact segment

$$\theta = \theta_l,\ M = M_l \equiv -\sin\theta_l / \sqrt{A B_{yy}(\theta_l)},\ Q_y = Q_{yl} \equiv -\sin\theta_l / B_{yy}(\theta_l). \tag{7}$$

The angle θ_i is one of the unknowns of this contact problem.

On the free segment the condition $Q_y = Q_{y0} - \tilde{w} s (Q_{y0} = \text{const})$ is fulfilled. Then from (3) we obtain the system of ordinary differential equations (ODE) for $M,\ \theta,\ x,\ y$; the general solution of this system contains four arbitrary constants. The boundary conditions have the form: at the fixed end (with $s = 0$) $x = y = 0,\ \theta = \theta_*$ (θ_* is the prescribed angle of fixation); at the free segment end (with $s = l$) conditions (7) and $y = h$. Altogether, to find the seven unknowns (among them $Q_{y0},\ l,\ \theta_l$) we set the seven boundary conditions.

We introduce the new coordinate $\xi \equiv l^{-1} s \in (0, 1)$ and write the resolving equations and boundary conditions with the use of this coordinate. The problem can be solved numerically by the finite difference method. For this purpose the rod is divided into N intervals with the uniform step $\delta = 1/N$. The differential equations and the boundary conditions are written in the difference form; grid functions $M_i,\ \theta_i,\ x_i,\ y_i\ (i = 0, ..., N)$ are placed in correspondence with the functions $M,\ \theta,\ x,\ y$ of continuous argument ξ. Using the approximate values at the nodes, the functions themselves are then recovered by interpolation [3, 8, 10, 18].

The system of ODEs is given in the operator form: $dY/d\xi = G(\xi, l, Y)$ where the function $Y = (M,\ \theta,\ x,\ y)^T$. To approximate the system we use implicit symmetric one-step difference scheme that has second order of accuracy [3, 10, 18]: $(Y_{i+1} - Y_i)/\delta = (G_i + G_{i+1})/2$, $(i = 0, ..., N-1)$. As a result of transformations we obtain the system of $4N$ difference nonlinear algebraic equations. Total number of unknowns consists of the values of the four desired functions at the nodes $4(N+1)$ and of the three additional constants $Q_{y0},\ l,\ \theta_l$. The system of equations is complemented with the difference analogues of seven boundary conditions: $x_0 = y_0 = 0,\ \theta_0 = \theta_*,\ y_N = h,,\ \theta_N = \theta_l,\ M_N = M_l,\ Q_{y0} = Q_{yl} + \tilde{w} l$. Then we apply the iteration method of Newton [3, 8, 18]. As an initial approximation we use the solution of a linear problem for the rod model in the classic formulation.

The outlined above algorithm was implemented in the software package MATHEMATICA. Also the problem was solved by the shooting method in the package MATHCAD (using the built-in functions `sbval` and `rkfixed`). The results agree.

The calculations is done for the pipeline which section is formed by two rings, internal steel and external concrete, with the radii $R_1 = 0.565$ m, $R_2 = 0.6$ m, $R_3 = 0.7$ m (see Fig. 1, b). These (and the following) parameters correspond the real pipeline of the company Nord Stream [1]. Steel has the elastic modulus $E_1 = 210$ GPa, the Poissons ratio is $\nu_1 = 0.28$, the volumetric mass density is $\rho_1 = 7800\ \text{kg/m}^3$. In this calculation concrete is considered as a physically linear material with the following properties: $E_2 = 27.5$ GPa, $\nu_2 = 0.2$, $\rho = 2450\ \text{kg/m}^3$ [9]. The density of sea water is $\rho_H = 1028\ \text{kg/m}^3$.

Defining the stiffnesses of pipeline as a compound rod, we consider that the steel and concrete layers operate parallel, therefore their stiffnesses are added:

$$A^{-1} = \sum_{n=1,2} E_n I_n,\ B_1{}^{-1} = \sum_{n=1,2} E_n S_n,\ B_2{}^{-1} = K \sum_{n=1,2} \mu_n S_n, \tag{8}$$

where the area of ring cross sections, their moments of inertia and shear moduli are calculated by formulas:

$$S_n \equiv \pi \left(R_{n+1}^2 - R_n^2\right),\ I_n \equiv \pi \left(R_{n+1}^4 - R_n^4\right)/4,\ \mu_n \equiv E_n/\left[2\left(1+\nu_n\right)\right]. \tag{9}$$

Here $n = 1, 2$ (index 1 refers to steel, 2 refers to concrete); $K = 0.5$ is the shear coefficient for the thin ring caused by the geometrical form of the cross section; the value of shear coefficient is defined in the study of boundary value problems, see [5].

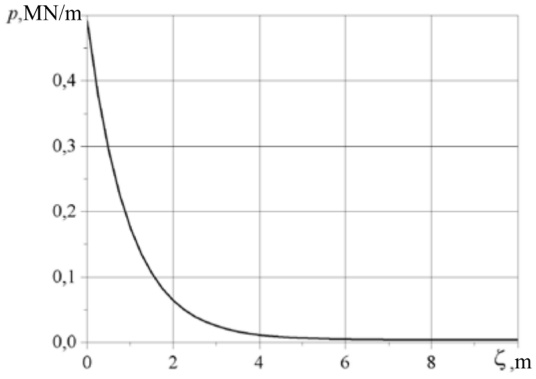

Fig. 2 Distribution of contact pressure ($\zeta = s - l$)

The calculation lets us evaluate the influence of tension and shear. The comparison of obtained results with the results of the Kirchhoffs model shows that the role of tension is negligible, and hence we can neglect the compliance B_1. The influence of shear is not large on the pipeline free segment: the contact point coordinate in the Kirchhoffs model is $x(l) = 265.4$ m, and in the model with shear it is 264.5 m; the values of force in the cross section corresponding to these models differ by fractions of a percent. But shear evidently affects the contact pressure (Fig. 2), because it is reduced to the concentrated force with $B_2 \to \infty$. The influence of shear on the bending moment is shown in Fig. 3 in the case when the depth and the angle of fixation are $h = 100\,\text{m},\ \theta_* = 30^o$. As we can see in the figures, the difference between the moment is small, however the model with shear gives us a nonzero value of moment at the beginning of the contact segment (Fig. 3, b).

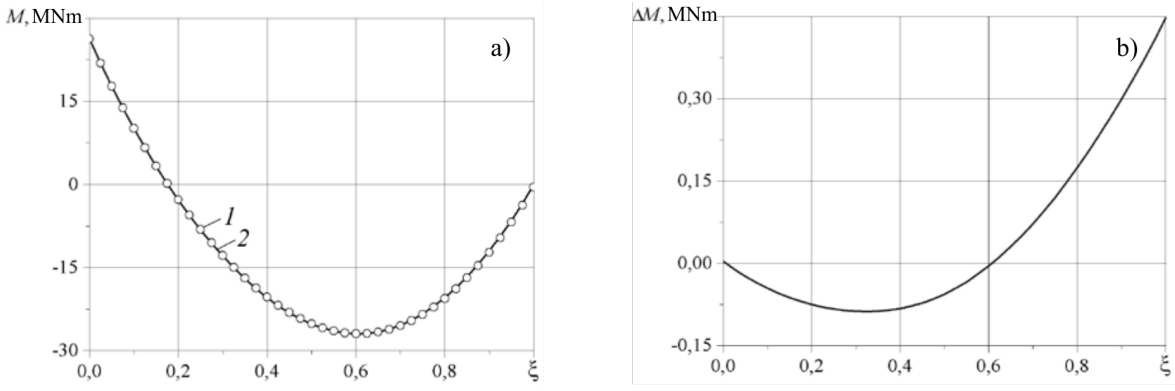

Fig. 3 Comparison of bending moment values calculated with two models. (a) Kichhoff's model (*line 1*), model with shear (*line 2*); difference of this moments (b)

Further we solve the problem with $\hat{\mathbf{B}}$ (i.e. the rod model problem in the classical formulation). With the help of this simpler model, we study the influence of the angle θ_* on the stress-strain state. Here we use the exact expression for the hydrostatic load.

4 Hydrostatic load

We consider the sagging segment of pipeline as a tube with the axis L and cross section F (Fig. 4). The position vector of points on the axis $\mathbf{r} = \mathbf{r}(s)$ is the function of arc coordinate. The unit vector $\mathbf{j}$ is directed along the axis y vertically down (as above). The pressure at the arbitrary point of tube surface (having the position vector $\mathbf{R}$) is equal $p = p_0 + \gamma \mathbf{j} \cdot \mathbf{R}$. Here p_0 is the pressure at $y = 0$ (Fig. 1), $\gamma = \rho_H g$ is the specific weight of water.

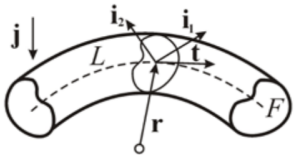

Fig. 4 Tube in water

On the part of tube $s_1 < s < s_2$ the hydrostatic forces act with the resultant vector

$$-\int\limits_O p\mathbf{N}dO = \int\limits_{s_1}^{s_2} \mathbf{q}_H ds. \tag{10}$$

Here O is the lateral surface, $\mathbf{N}$ is the external normal unit vector to this surface. We are faced with derivation of the expression of hydrostatic load $\mathbf{q}_H$ distributed per unit length.

We define the vector of area $\mathbf{N}dO$ by well-known means of differential geometry. In every section $s =$ const we introduce the Cartesian axes x_α with the unit vectors $\mathbf{i}_\alpha$. On the contour ∂F of the section we have the functions of arc coordinate $x_\alpha = x_\alpha(\omega)$. The tube surface is given by the dependence of position vector on two coordinates $\mathbf{R}(\omega, s) = \mathbf{r}(s) + \mathbf{x}$, $\mathbf{x} \equiv x_\alpha(\omega)\mathbf{i}_\alpha(s)$. Along the tangents to coordinate lines we direct the vectors of derivatives $\mathbf{R}_\omega \equiv \partial\mathbf{R}/\partial\omega = x_\alpha{}'(\omega) \cdot \mathbf{i}_\alpha \equiv \boldsymbol{\tau}$, $\mathbf{R}_s \equiv \partial\mathbf{R}/\partial s = \mathbf{t} + \boldsymbol{\Omega}^0 \times \mathbf{x}$ ($\mathbf{r}'(s) = \mathbf{t}$, $\mathbf{i}_\alpha{}'(s) = \boldsymbol{\Omega}^0 \times \mathbf{i}_\alpha$) (prime denotes the derivatives of function of one argument). We introduce the tangent unit vectors to the contour $\boldsymbol{\tau}$ and to the axis $\mathbf{t}$ and also the vector of curvature and twisting of the tube $\boldsymbol{\Omega}^0$. Then the normal unit vector to the contour in the section plane is defined as $\mathbf{n} = \boldsymbol{\tau} \times \mathbf{t}$ and the area vector on the tube surface is $\mathbf{N}dO = \mathbf{R}_\omega \times \mathbf{R}_s d\omega ds = \left[\mathbf{n} + \boldsymbol{\tau} \times \left(\boldsymbol{\Omega}^0 \times \mathbf{x}\right)\right] d\omega ds$. We substitute these expressions into (6) and obtain $\mathbf{q}_H = -\oint\limits_{\partial F} p\left[\mathbf{n} + (\mathbf{t} \times \mathbf{n}) \times \left(\boldsymbol{\Omega}^0 \times \mathbf{x}\right)\right] d\omega$.

Next we take into account the dependence $p(y)$ and use the generalized divergence theorem (in the section plane): $\oint\limits_{\partial F} n_\alpha W d\omega = \int\limits_F \partial_\alpha W dF$ ($\partial_\alpha \equiv = \partial/\partial x_\alpha$). Assuming $\int x dF = 0$ (i.e. the tube axis passes through the centers of gravity), we obtain the desired expression of hydrostatic load:

$$\mathbf{q}_H = F\left[-\gamma \mathbf{j}_\perp + (p_0 + \gamma y)\mathbf{t}'\right] \tag{11}$$

where $\mathbf{j}_\perp = \mathbf{j} - \mathbf{j} \cdot \mathbf{tt}$ is the part of the unit vector $\mathbf{j}$ in the section plane. We note that vector $\mathbf{t}'(s)$ is directed along the principal normal to the tube axis, and its module is equal to the curvature of the axis.

We can obtain formula (7) using a simpler way [14, 19, 22]. The elementary derivation is based on the Archimedes principle for the element of the tube between the cross sections s and $s + ds$:

$$-\gamma F \mathbf{j} ds = \mathbf{q}_H ds - F p\, \mathbf{t}\big|_s^{s+ds},\ p = p_0 + \gamma \mathbf{j} \cdot \mathbf{r} \Rightarrow \mathbf{q}_H = F\left[-\gamma \mathbf{j} + (p\mathbf{t})'\right] = F\left[-\gamma(\mathbf{j} - \mathbf{j} \cdot \mathbf{tt}) + p\mathbf{t}'\right]. \tag{12}$$

Though unlike the presented above more general derivation, this way cannot be used beyond the scope of hydrostatics (when the pressure is defined by the integrals of Bernoulli or Lagrange–Cauchy).

5 Pipeline as Kirchhof's rod

Let us turn to the problem of the pipeline deformation in laying process in the case of action of hydrostatic load (7) and $\hat{\mathbf{B}} = 0$. We follow from the vector equations to the projections in the basis $\mathbf{e}_\alpha$. We take use of the equations $\equiv Q_\alpha \mathbf{e}_\alpha$, $\mathbf{e}_1{}' = \theta' \mathbf{e}_2$, $\mathbf{e}_2{}' = -\theta' \mathbf{e}_1$, $\mathbf{q} = w\mathbf{j} + \mathbf{q}_H$ (here w is the pipeline weight distributed per unit length) from (1), get

$$\begin{aligned} &Q_1{}' - \theta' Q_2 = -q_1 = -w \sin\theta, \\ &Q_2{}' + \theta' Q_1 = -q_2 = -(w - F\gamma)\cos\theta - F(p_0 + \gamma y)\,\theta', \\ &M' = -Q_2,\ \theta' = AM,\ x' = \cos\theta,\ y' = \sin\theta \end{aligned} \tag{13}$$

and write the boundary conditions: $s = 0:\ x = y = 0,\ \theta = \theta_*$; $s = l:\ y = h,\ \theta = 0,\ Q_l = 0,\ M = 0$. On the contact segment of pipeline and bottom we have the undeformed state. The value $Q_2(l-0)$ is equal to the concentrated contact force with negative sign.

The computations are done with the same parameters as above (see Sect. 3). In Fig. 5 we present the graphs of axial and transverse forces and also of bending moment for the various depth values h. These results are obtained with the two expressions of hydrostatic load, exact (7) and simplified; the angle of fixation is $\theta_* = 30^o$. We see that, in comparison with the approximated load, the use of exact hydrostatic load changes significantly the picture of internal loads in the pipeline. The calculations reveal the large tension force at the attaching point. The simplified model of liquid weight gives value of next lower order (8 times smaller for the depth 250 m). The pipeline vessel has to provide this force for the holding of sagging pipeline. Insufficient tension leads to exceeding bending and destruction even for shallow areas.

6 Consideration of physical nonlinearity of concrete

Deformations of the pipeline are significant; therefore we need to take into account the physical nonlinearity characteristic to concrete [9]. We show in Fig. 6 the stress-strain curve of concrete with the uniaxial tension-compression. The dependence of the stress σ on the strain ε is approximated by the cubic function: $\tilde{\sigma}(\varepsilon) = E\varepsilon + K_1\varepsilon^2 + K_2\varepsilon^3$, where $K_1 = -E\left(\varepsilon_1^{-1} + \varepsilon_2^{-1}\right)/2$, $K_2 = E\varepsilon_1^{-1}\varepsilon_2^{-1}/3$. However outside the interval $(\varepsilon_1,\ \varepsilon_2)$ the dependence must be corrected on the grounds of keeping the stability of material [7]. We take

$$\sigma(\varepsilon) = \begin{cases} \sigma_1, & \varepsilon < \varepsilon_1, \\ \tilde{\sigma}(\varepsilon), & \varepsilon_1 \le \varepsilon \le \varepsilon_2, \\ \sigma_2, & \varepsilon > \varepsilon_2. \end{cases} \tag{14}$$

Without going into details of the three-dimensional rod modeling [4–6, 21], we restrict ourselves by the elementary considerations of beam bending [5]. In this case the strain is linearly distributed across the thickness: $\varepsilon = -\kappa\eta$, $\eta \in (-H, H)$ (η is the Cartesian coordinate in the cross section, $2H$ is the section height). If the section is symmetric with respect to the vertical axis η and if $b(\eta)$ is its width, then bending moment equals

$$M_2(\kappa) = -\int_{-H}^{H} \sigma(-\kappa\eta)\,\eta\, b(\eta)\, d\eta. \tag{15}$$

For the concrete ring (see Fig. 1, b) the function $b(\eta)$ has the form

$$b(\eta) = 2\begin{cases} \sqrt{R_3^2 - \eta^2}, & R_2 \le |\eta| \le R_3, \\ \sqrt{R_3^2 - \eta^2} - \sqrt{R_2^2 - \eta^2}, & 0 \le |\eta| < R_2. \end{cases} \tag{16}$$

By summing M_2 and the moment in the steel tube we find the bending moment in pipeline: $M(\kappa) = E_1 I_1 \kappa + M_2(\kappa) \Rightarrow \kappa = \kappa(M)$. The last inverse function is substituted into the system (9) (instead of $\theta' = AM$).

Figure 7 contains the results of calculation for $M_2(\kappa)$ and $\kappa(M)$. The dashed line depicts the linear concrete model. The graphs are obtained with the set of parameters: $\sigma_1 = -15$ MPa, $\sigma_2 = 1,35$ MPa, $\varepsilon_1 = -4,27 \cdot 10^{-4}$, $\varepsilon_2 = 9,16 \cdot 10^{-5}$ [9].

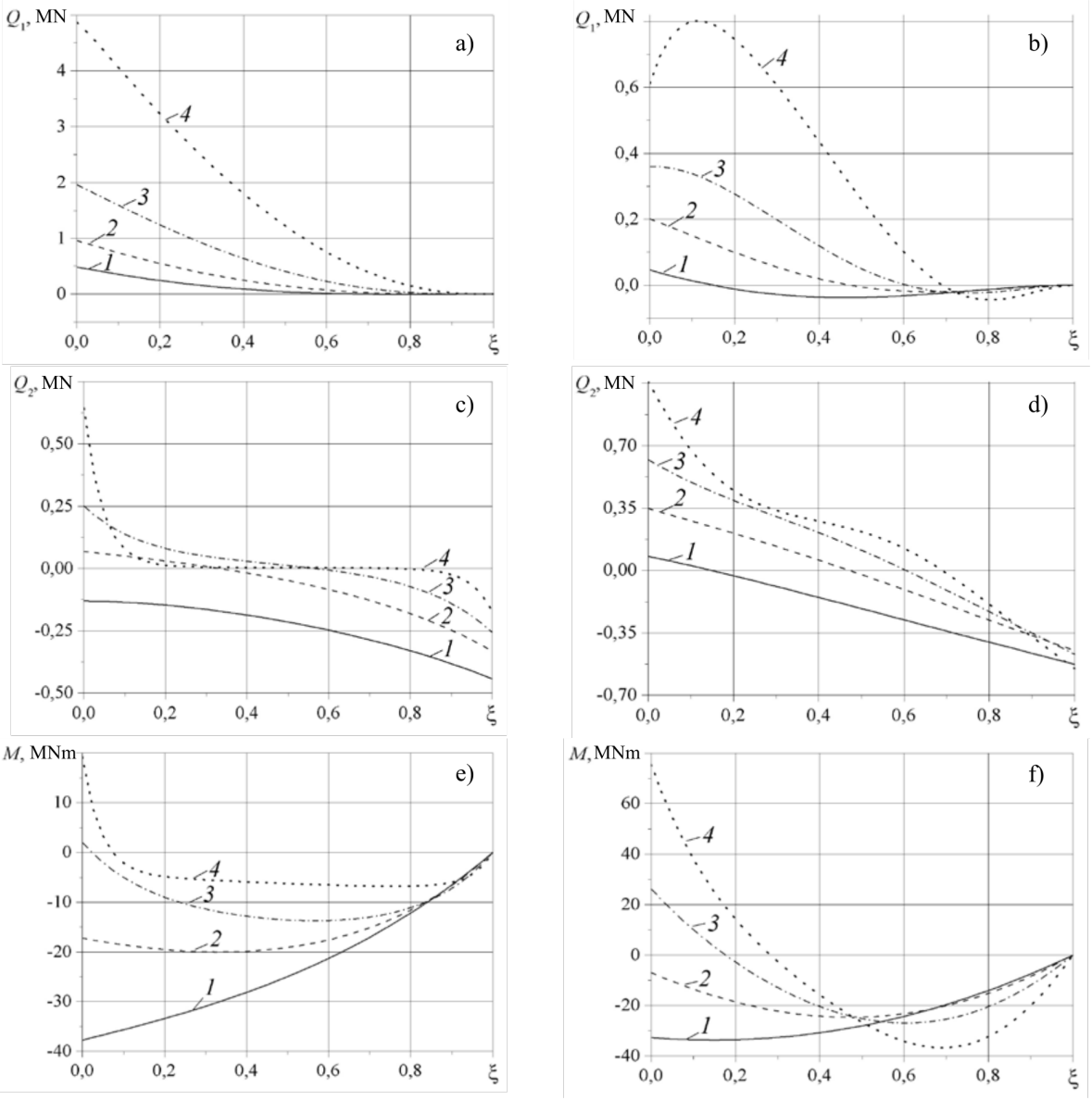

Fig. 5 Axial Q_1 and transverse Q_2 forces, bending moment M in pipeline for various values of depth θ_*: 30 m, (*lines 1*), 50 m (*2*), 100 m (*3*), 250 m (*4*) with exact (a, c, e) and simplified (b, d, f) consideration of hydrostatic load

7 Influence of initial angle, of nonlinearity of concrete, and of depth

Numerical results with taking into account the physical nonlinearity of concrete is shown in Fig. 8. We draw the form of sagging segment of pipeline and the internal forces for the various fixation angle values θ_* with the depth of laying $h = 100$ m. The influence of physical nonlinearity is shown by an example of bending moment (Fig. 8 d).

After determination of the forces and moments in the compound pipeline-rod we need to evaluate the arising stresses. Staying within the elementary considerations and assuming the fulfillment of Hookes law for concrete, we obtain the following expressions for the maximal (in section) stresses in steel (index s) and in concrete (index c):

$$\sigma_s = Q_1 / [S_1 (1+\alpha)] + |M| R_2 / [I_1 (1+\beta)], \tag{17}$$

$$\alpha \triangleq (E_2 S_2) / (E_1 S_1), \; \beta \triangleq (E_2 I_2) / (E_1 I_1), \tag{18}$$

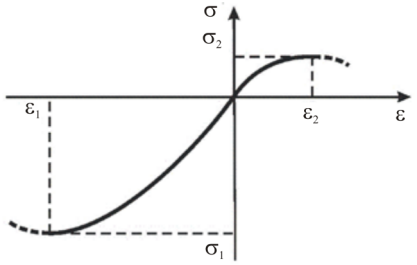

Fig. 6 Stress-strain curve

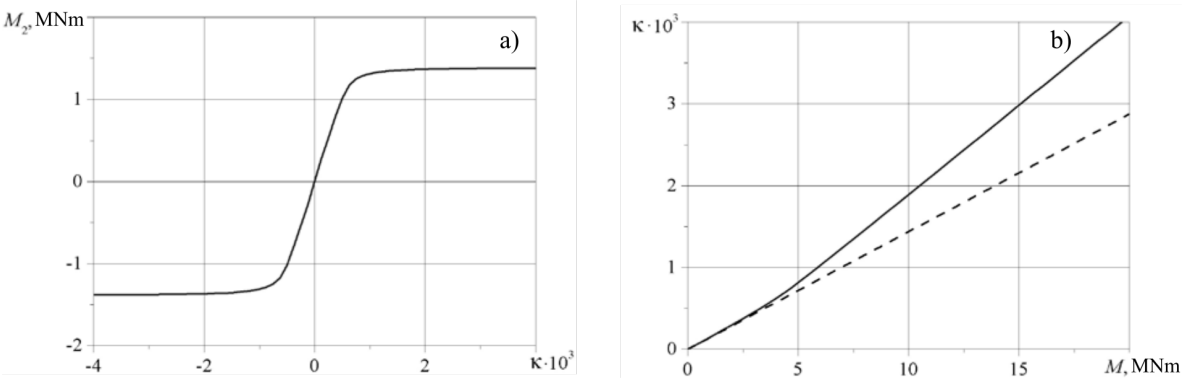

Fig. 7 (a) Bending moment in concrete tube and (b) dependence of curvature on moment

Table 1 Dependence of optimum fixation angle on depth

Laying depth h, m	0–10	10–30	30–70	70–140	140–300
Laying angle θ_*, grad	0	10	20	30	35

$$\sigma_c = Q_1 / \left[S_2 \left(1 + \alpha^{-1}\right)\right] + |M| R_3 / \left[I_2 \left(1 + \beta^{-1}\right)\right]. \tag{19}$$

The dependence of maximal stress in steel on laying depth h with the various fixation angles θ_* is shown in Fig. 9. We see what angle should be chosen for laying the pipeline so that the yield stress of steel $[\sigma_l] =$ 400 MPa is not exceeded.

On the basis of the obtained results we can establish the optimum relation between the depth and the angle of pipeline laying. So, with reaching the certain depth values one should increase the angle θ_*, otherwise the stresses in steel increase inadmissibly. The optimum fixation angles for the depth up to 300 m are shown in the table.

The dependence of maximum stresses in concrete is analogous to the one depicted in Fig. 9, but the stress values are approximately seven times lower, than in steel. Calculations reveal that in the whole considered diapason of depths and angles the stresses reach the yield stresses of concrete tension $[\sigma_2] = 1,35$ MPa, and it occurs simultaneously in almost all sections of the sagging segment of pipeline.

8 Conclusion

We developed the mathematical model of the underwater pipeline as a nonlinear-elastic rod. We determined the hydrostatic load on the pipeline. We formulated and solved (with account for various factors) the contact problems of deformation arising in laying process. We made recommendations to optimize the process to reduce the loads on the vessel and the stresses in the tube.

References

1. Nord Stream: construction. URL http://www.nord-stream.com/ru/gazoprovod/cozdanie/

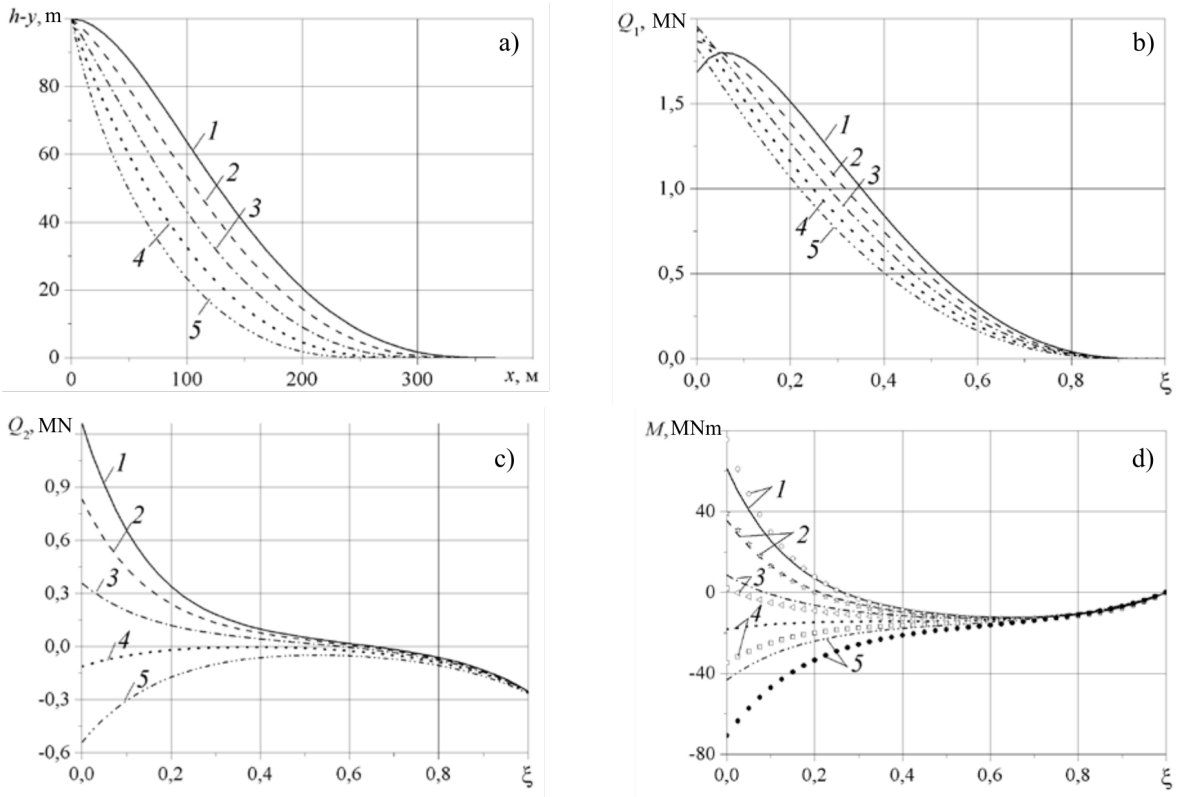

Fig. 8 Dependences of form of pipeline sagging segment (a); of axial (b) and of transverse (c) forces, of bending moment (d) on fixation angle θ_*: 0 (*lines 1*), 15 (*2*), 30 (*3*), 45 (*4*), 60 (*5*) with laying depth $h = 100$ m; in fragment 8 (d) similar dependences without physical nonlinearity are shown

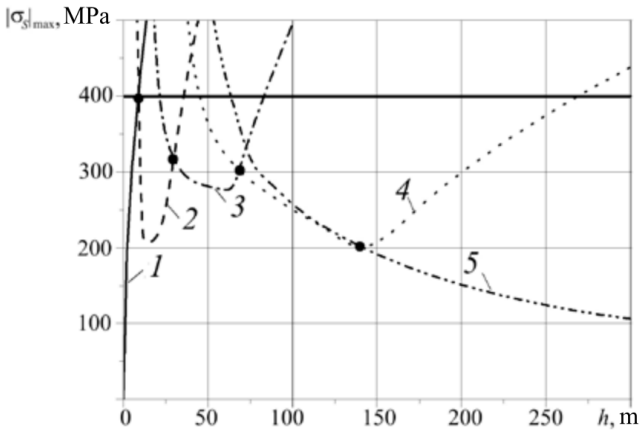

Fig. 9 Dependence of maximal stress in steel on laying depth h with various values of fixation angle θ_*: 0 (*line 1*), 10 (*2*), 20 (*3*), 30 (*4*), 35 (*5*)

Fig. 10 Scheme of pipeline and its section. 1 is steel, 2 is concrete

2. Antman, S.: Nonlinear problems of elasticity. Springer, New York (2005). DOI 10.1007/0-387-27649-1
3. Bahvalov, N.S., Zhidkov, N.P., Kobelkov, G.G.: Numerical methods. Binom. Laboratoria znanii, Moscow (2003)
4. Eliseev, V.: Mechanics of elastic bodies. St.-Peterbg. State Polytech. Univ. Publ. House, St. Petersburg (2003)
5. Eliseev, V.: Mechanics of deformable solid bodies. St.-Peterbg. State Polytech. Univ. Publ. House, St. Petersburg (2006)
6. Eliseev, V.V., Zinovieva, T.V.: Mechanics of thin-walled structures. Theory of rods. St. Petersburg State Polytech. Univ. Publ. House, St. Petersburg (2008)
7. Kachanov, L.M.: Foundations of theory of plasticity. Nauka, Moscow (1969)
8. Kahaner, D., Moler, C., Nash, S.: Numerical methods and software. Prentice-Hall, New Jersey (1989)
9. Karpenko, N.I.: General models of reinforced concrete. Stroyizdat, Moscow (1996)
10. Kiryanov, D., Kiryanova, E.: Computational science. Infinity Science Press, Hingham (2007)

11. Kyriakides, S., Corona, E.: Mechanics of offshore pipelines. Vol. 1: Buckling and collapse. Elsevier, Slovenia (2007)
12. Lenci, S., Callegari, M.: Simple analytical models for the j-lay problem. Acta Mech. **178**(1–2), 23–29 (2005). DOI 10.1007/s00707-005-0239-x
13. Mossakovskii, V.I., Gudramovich, V.S., Makeev, E.M.: Contact problems of theories of shells and rods. Mashinostroyenie, Moscow (1978)
14. Pedersen, P.T.: Equilibrium of offshore cables and pipelines during laying. Int. Shipbuilding Progress **22**(256), 399–408 (1975)
15. Popov, E.P.: Theory and calculation of flexible elastic rods. Nauka, Moscow (1986)
16. Raman-Nair, W., Baddour, R.E.: Three-dimensional dynamics of a flexible marine riser undergoing large elastic deformations. Multibody System Dyn. **10**(4), 393–423 (2003). DOI 10.1023/A:1026213630987
17. Rienstra, S.W.: Analytical approximations for offshore pipelaying problems. In: Proc. I Conf. Industrial & Applied Math., pp. 99–108. CWI Tracts, Amsterdam (1987)
18. Samarskii, A.A., Gulin, A.V.: Numerical methods. Nauka, Moscow (1989)
19. Stump, D.M., van der Heijden, G.H.M.: Matched asymptotic expansions for bent and twisted rods: applications for cable and pipeline laying. J. Eng. Math. **38**(1), 13–31 (2000). DOI 10.1023/A:1004634100466
20. Svetlitskii, V.A.: Dynamics of rods. Springer, Berlin–Heidelberg (2005). DOI 10.1007/b137699
21. Vetyukov, Y.M., Eliseev, V.V.: Modelling of building frames as spatial rod structures with geometric and physical nonlinearity. Comp. Cont. Mech. **3**(3), 32–45 (2010)
22. Zinovieva, T.V.: Analysis of pipeline stress-strain state in seabed laying. Neftegazovoe Delo (1), 220–236 (2011). URL http://www.ogbus.ru/authors/Zinovieva/Zinovieva_1.pdf

View publication stats